Indonesian Journal of Material Research
e-ISSN: 2987-1654
Vol. 2, No. 2, July 2024

Indonesian Journal of MATERIAL RESEARCH

Research Paper

Efficient Adsorption of Cr(VI) from Aqueous Solutions Using Composites Modified with Ni/Al LDH and Keggin Type Compounds

Normah Normah[1]*, Nurmalina Adhiyanti[1], Rabellia Juladika Sayeri[2], Alfan Wijaya[2]

[1] *Departement of Chemistry, Universitas Indo Global Mandiri, Palembang, 30129, Indonesia*
[2] *Research Center of Inorganic Materials and Coordination Complexes, Sriwijaya University, Palembang, 30139, Indonesia*
***Corresponding author**: normah@uigm.ac.id

Abstract
This study aims to synthesize the NiAl-LDH/$K_4[\alpha\text{-}SiW_{12}O_{40}]$ composite using the coprecipitation method and evaluate its ability to adsorb Cr(VI) from aqueous solutions. The material characterization showed a significant increase in the specific surface area of the composite compared to pure NiAl-LDH, contributing to an enhanced Cr(VI) adsorption capacity. XRD and FT-IR results confirmed the successful synthesis and integration of $K_4[\alpha\text{-}SiW_{12}O_{40}]$ into the NiAl-LDH structure. At the same time, BET analysis indicated that the specific surface area of the composite doubled compared to pure NiAl-LDH. The adsorption kinetics data indicated that the adsorption process followed the Pseudo-Second-Order (PSO) model with an R^2 value close to 1, suggesting the dominance of chemisorption in the Cr(VI) adsorption mechanism. Isotherm analysis showed that the Freundlich model was more suitable than the Langmuir model, indicating that adsorption occurred on a heterogeneous surface with multilayer formation. The Cr(VI) adsorption capacity of the NiAl-LDH/$K_4[\alpha\text{-}SiW_{12}O_{40}]$ composite reached 17.123 mg/g, higher than that of pure NiAl-LDH at 188.68 mg/g. The Cr(VI) adsorption process involved chemical interactions between Cr(VI) and functional groups on the adsorbent surface, complex formation, and precipitation.

Keywords
Composite NiAl-LDH, Keggin Type Compound, Adsorption, Cr(VI)

Received: 29 April 2024, Accepted: 16 July 2024
https://doi.org/10.26554/ijmr.20242228

1. INTRODUCTION

Hexavalent chromium, or chromium(VI), is a highly hazardous and carcinogenic contaminant frequently in industrial effluents. Because of the severe threats it causes to the environment and public health when present in water bodies, efficient removal techniques must be developed. Adsorption is one of the many strategies that has attracted much interest because of its ease of use, affordability, and high efficiency (Babapour et al., 2022; Setyawan et al., 2024).

Layered double hydroxides (LDHs) have emerged as promising materials for environmental applications, particularly in adsorption processes. LDH has the potential to be applied in the environment, energy, and biomedical. LDH are called multi-metal clay materials and exhibit layered structures resembling hydrotalcite/brucite in 2D. LDHs consist of divalent and trivalent metal cations, with the general formula $[M^{II}_{1-x}M^{III}_{x}(OH)_2]^{x+}\cdot[An^{-}x/n.mH_2O]$ (which, M^{II} represents divalent metallic cations such as Ni, Ca, Mg, Zn, Cu; M^{III} includes trivalent metallic cations such as Al, Fe, Cr; An^{-} indicating negatively charged interlayer LDHs anions) (Bai et al., 2024; Daud et al., 2019; Ding et al., 2024; Mutahir et al., 2024; Zhao et al., 2023). Octahedral layers, adopting a brucite-like structure reminiscent of $Mg(OH)_2$, form the foundation of these materials. The characteristics of LDHs make them highly promising for applications as catalysts and adsorbents in wastewater treatment, owing to their straightforward preparation process. (Deng et al., 2021; Gu et al., 2024; Latuconsina, 2010; Qian et al., 2023; Zarei et al., 2023). In addition to their effectiveness in wastewater treatment, LDHs demonstrate excellent adsorption capabilities for various inorganic and organic pollutants, including dyes, metals, pesticides, phosphates, and CO_2 (Farhan et al., 2024).

LDHs are commonly synthesized using inorganic salts and the addition of water or organic solvents. Achieving optimal results necessitates precise control of both pH and temperature to induce precipitation and crystal growth (Cao et al., 2023). The LDHs formed under these controlled conditions exhibit a distinctive 2D layered structure (Boccalon et al., 2020). Layered LDH structures, synthesized through a combination of multi-metal compositions and interlayer anions, can confer desirable properties such as enhanced surface area, phase purity, porosity, and crystallinity (Daniel et al., 2023; Nie et al., 2023; Wang et al., 2023b). Furthermore, LDHs showcase unique characteristics, including high chemical stability, ion exchange capability, struc-

ture memory effect, reactive interlayer space, catalytic activity, specific surface area, biocompatibility, and modifiable hydroxide layer or structural interlayer composition (Bouali et al., 2020; Boulaiche et al., 2019; Jiang et al., 2024; Wang et al., 2023b)

Numerous reports in the literature delve into the modification of LDHs, employing various techniques. Intercalation methods, exemplified by Xu et al. (2024) and Chen et al. (2024), and composite approaches, researched by Gu et al. (2024), Jiang et al. (2024), and Kumari et al. (2024) represent key strategies in research development. In a specific application, Mg-Al LDHs were modified by intercalating nitrate ions into the LDH interlayer, serving as an effective adsorbent for removing methyl orange dyes (Yadav and Dasgupta, 2022). Based on the research by Elanchezhiyan and Meenakshi (2017) synthesized a chitosan/Mg-Al composite using the coprecipitation method in a study that enhanced adsorption capacity. When employed as an adsorbent for removing oil particles from oil-in-water emulsions, this composite exhibited a remarkable adsorption capacity of 78%, a substantial improvement compared to pure LDH (30%). The mechanism of the adsorption was attributed to hydrophobic-hydrophobic interactions. In summary, these findings highlight the diverse modification techniques for LDHs and showcase the promising application of the chitosan/Mg-Al composite for efficient oil particle removal through enhanced adsorption capacity.

Based on our previous research involving the modification of LDH, which showed promising results in removing Cr(VI) metal. this research aims to prepare a NiAl-LDH/$K_4[\alpha\text{-}SiW_{12}O_{40}]$ composite. The composite will be synthesized using the coprecipitation method. This composite is expected to enhance the effectiveness of Cr(VI) removal from aqueous solution.

2. EXPERIMENTAL SECTION

2.1 Materials and Instrumentals

Nickel(II) nitrate trihydrate ($Ni(NO_3).3H_2O$), Aluminum(III) nitrate nonahydrate ($Al(NO_3)_3.9H_2O$), sodium tungstate (Na_2WO_4, 99.99%), sodium phosphate (NaH_2PO_4, 99%), and potassium chloride (KCl, 99%) were purchased from Sigma Aldrich. Hydrochloric acid (HCl) (purity = 37%) and sodium hydroxide (NaOH) were obtained from Merck. Potassium dichromate ($K_2Cr_2O_7$) and 1,5-Diphenylcarbazide ($C_{13}H_{14}N_4O$) for the adsorption process were obtained from LOBA Chemie. All chemicals were utilized without further purification. Distilled water was used for the synthesis and adsorption experiments. To learn more about the material's physicochemical characteristics, several spectroscopic approaches were used to characterize composite NiAl-LDH/$K_4[\alpha\text{-}SiW_{12}O_{40}]$ samples. With the Rigaku MiniFlex-6000 XRD, X-ray diffraction patterns were captured utilizing CuK α radiation at a scan speed of 10,000 degrees per minute. A Shimadzu Prestige-21 FT-IR spectrometer was used to evaluate the FT-IR spectra. Quantachrome Micromeritics ASAP version 3.01 was used for the BET analysis to calculate the materials' surface area, pore volume, and pore diameter.

2.2 Methods

2.2.1 Synthesis of $K_4[\alpha\text{-}SiW_{12}O_{40}]$ Compound Powder

Powdered polyoxometalate compounds can be prepared by dissolving two grams of sodium phosphate in one hundred milliliters of distilled water (Silaen et al., 2021). After 12 grams of tungstate solution were dissolved in 300 milliliters of boiling water and strong choride acid, the mixture was added. The mixture was stirred at 50°C throughout the day. Next, it was treated with 50 grams of potassium chloride and dried for 5 hours at 50°C.

2.2.2 Preparation of NiAl-LDH/$K_4[\alpha\text{-}SiW_{12}O_{40}]$ Composite

This has been done using the NiAl-LDH/$K_4[\alpha\text{-}SiW_{12}O_{40}]$ composite coprecipitation method (Palapa et al., 2021). The aluminum(III) and nickel(II) nitrate solutions were first combined in a molar ratio of 3:1. Next, 2 M sodium hydroxide solution was added until the pH of the mixture reached 10. $K_4[\alpha\text{-}SiW_{12}O_{40}]$ compound Powder was added after being dissolved in 50 milliliters of distilled water and allowed to settle. Nitrogen gas is added to the mixture and allowed to sit throughout the day. After a precipitate is formed, filtered and dried for 12 hours at 60°C. The green material is then ground into powder using a mortar and pestle.

2.2.3 Adsorption Measurement

Cr(VI) metal adsorption experiments were carried out using a 3 mg/L standard solution concentration. The adsorption experiment aims to determine the effect of pH, temperature, contact time between adsorbent and adsorbate, and concentration. Each experiment involved 30 mg of adsorbent placed in a 250 mL beaker, to which 30 mL of a 30 mg/L adsorbate solution was added. The pH of the solution varied from 2 to 10. The effect of contact time was studied at 10-minute intervals.

The final concentration of Cr(VI) metal adsorbate was determined using UV-Vis spectrophotometry at the maximum wavelength (543 nm). The effect of concentration was explored by varying temperature (30, 40, 50, 60°C) and initial adsorbate concentration (ranging between 5, 10, 15, 20, and 25 mg/L), with 30 mg of adsorbent used in a 250 mL beaker. Separately for each condition.

3. RESULTS AND DISCUSSION

3.1 Material Characterization

Figure 1 presents the X-ray diffraction (XRD) patterns of the NiAl-LDH/$K_4[\alpha\text{-}SiW_{12}O_{40}]$ composite preparation, alongside comparisons with NiAl-LDH and $K_4[\alpha\text{-}SiW_{12}O_{40}]$ compound. The XRD patterns of these three materials exhibit strong crystallinity, with peaks observed in both NiAl-LDH/$K_4[\alpha\text{-}SiW_{12}O_{40}]$ and pure NiAl-LDH, consistent with the JCPDS standard (Normah et al., 2021b; Wibiyan et al., 2024). Incorporating the $K_4[\alpha\text{-}SiW_{12}O_{40}]$ compound modifies some peak angles and intensities observed in the NiAl-LDH/$K_4[\alpha\text{-}SiW_{12}O_{40}]$ composite, which combines characteristics of both NiAl-LDH and $K_4[\alpha\text{-}SiW_{12}O_{40}]$ compound.

Distinct features in the XRD pattern of NiAl-LDH/$K_4[\alpha\text{-}SiW_{12}O_{40}]$ composite are observed around 8.42°, 10°, and between 20-30° angles. The NiAl-LDH characteristics at 10°, 24°, 35°, and

61° are evident in the XRD pattern of NiAl-LDH/ $K_4[\alpha\text{-}SiW_{12}O_{40}]$ composite, while new peaks at 8°, 20°, and 25-30° are attributed to the $K_4[\alpha\text{-}SiW_{12}O_{40}]$ compound. This study indicates an increase in interlayer spacing from 7.41 Å (11.94°) in NiAl-LDH to 10.53 Å (8.42°) in NiAl-LDH/$K_4[\alpha\text{-}SiW_{12}O_{40}]$, suggesting the incorporation of the $K_4[\alpha\text{-}SiW_{12}O_{40}]$ compound (Li et al., 2017; Niatouri and Yadollahi, 2023).

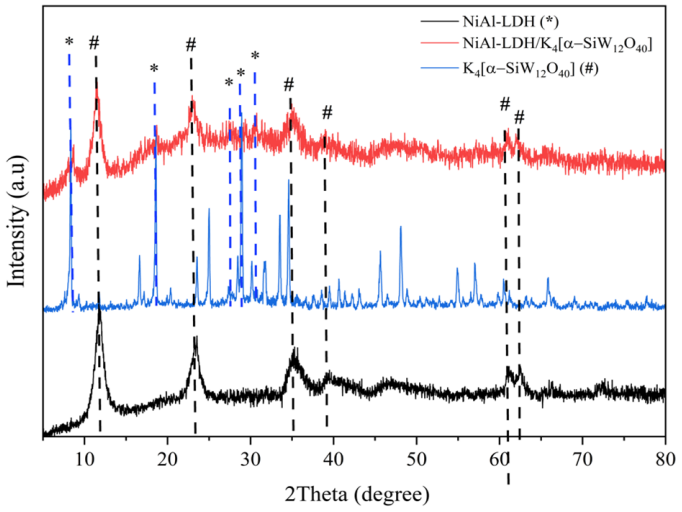

Figure 1. The XRD Patterns of the NiAl-LDH, $K_4[\alpha\text{-}SiW_{12}O_{40}]$] Compound, and NiAl-LDH/$K_4[\alpha\text{-}SiW_{12}O_{40}]$ Composite

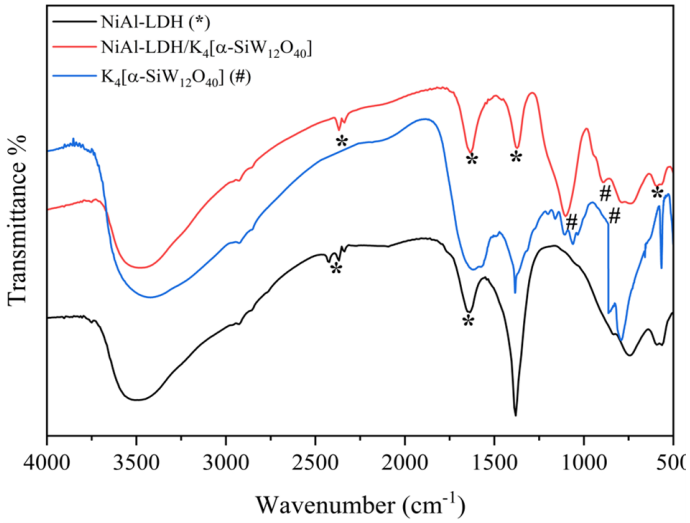

Figure 2. FT-IR Spectra NiAl-LDH, $K_4[\alpha\text{-}SiW_{12}O_{40}]$ Compound, and NiAl-LDH/$K_4[\alpha\text{-}SiW_{12}O_{40}]$ Composite

The Fourier Transform Infrared (FT-IR) spectroscopy analysis, depicted in Figure 2, identifies the various chemical bonds and molecular interactions within the NiAl-LDH/$K_4[\alpha\text{-}SiW_{12}O_{40}]$ composite by examining infrared light absorption at different wavelengths. The composite's FT-IR spectrum features characteristic peaks corresponding to the NiAl-LDH and the $K_4[\alpha\text{-}SiW_{12}O_{40}]$ compound. Specifically, the vibrational peaks at 1103 cm^{-1} (Si−O−Si) and 894 cm^{-1} (W−O−W) indicate the presence of the $K_4[\alpha\text{-}SiW_{12}O_{40}]$ compound. The vibrational peak at 3502 cm^{-1} corresponds to the interlayer O−H anions found in LDH. In comparison, the peak at 1635.64 cm^{-1} corresponds to the bending vibrations of H−O−H bonds, likely due to water molecules within the LDH structure. The peak at 1381 cm^{-1} also suggests stretching vibrations of various anions within the composite. Metal-oxygen bond vibrations are indicated by peaks at 747 cm^{-1} (Al−O) and 563 cm^{-1} (O−Ni−O), confirming the presence of aluminum and nickel within the LDH structure (Hanifah and Amri, 2023; Li et al., 2017). The FT-IR spectrum thus confirms the successful incorporation of the $K_4[\alpha\text{-}SiW_{12}O_{40}]$ compound into the NiAl-LDH matrix, retaining structural features from both components and indicating successful composite formation.

Figure 3 shows the N_2 adsorption-desorption isotherm curve of the material. The calculation of specific surface area indicates a significant increase in the NiAl-LDH/$K_4[\alpha\text{-}SiW_{12}O_{40}]$ composite. The specific surface area (Table 1) obtained is as follows: NiAl-LDH is 58.11 m^2/g, and NiAl-LDH/$K_4[\alpha\text{-}SiW_{12}O_{40}]$ composite is 116.16 m^2/g. These results indicate that the modification of LDH can enhance the structural characteristics of LDH, with the addition of $K_4[\alpha\text{-}SiW_{12}O_{40}]$ compound material to NiAl-LDH, increasing the surface area by two-fold. This finding is consistent with XRD analysis results showing that LDH modification increases interlayer spacing and surface area.

Table 1. The Characteristics Adsorbent of NiAl-LDH and NiAl-LDH/$K_4[\alpha\text{-}SiW_{12}O_{40}]$ Composite

Adsorbent	S_{BET} (m^2/g)	V_p (cm^3/g)
NiAl-LDH	58.11	0.12
NiAl-LDH/$K_4[\alpha\text{-}SiW_{12}O_{40}]$ composite	116.16	0.23

3.2 Adsorption Experimental

Figure 4 and Table 2 illustrate the adsorption mechanism of NiAl-LDH and the NiAl-LDH/$K_4[\alpha\text{-}SiW_{12}O_{40}]$ composite based on kinetic parameters. Figure 4 shows that the adsorption quantity increases with the contact duration. NiAl-LDH has an adsorption capacity of 1.668 mg/g, while the NiAl-LDH/$K_4[\alpha\text{-}SiW_{12}O_{40}]$ composite has an adsorption capacity of 2.228 mg/g. Interestingly, the adsorption capacity of both materials increases significantly. In the adsorption of Cr(VI) metal by NiAl-LDH and the NiAl-LDH/$K_4[\alpha\text{-}SiW_{12}O_{40}]$ composite, the large surface area and the presence of suitable functional groups on the material's surface allow solid interactions and the formation of chemical bonds with Cr(VI) ions, resulting in high adsorption capacities.

Pseudo-first-order (PFO) and pseudo-second-order (PSO) models were used to study the adsorption kinetics (Taher et al., 2024; Wang et al., 2023a). The results of the analysis are shown in Table 2. The data indicate that the adsorption process of the adsorbent follows the PSO model, evidenced by the coefficient of

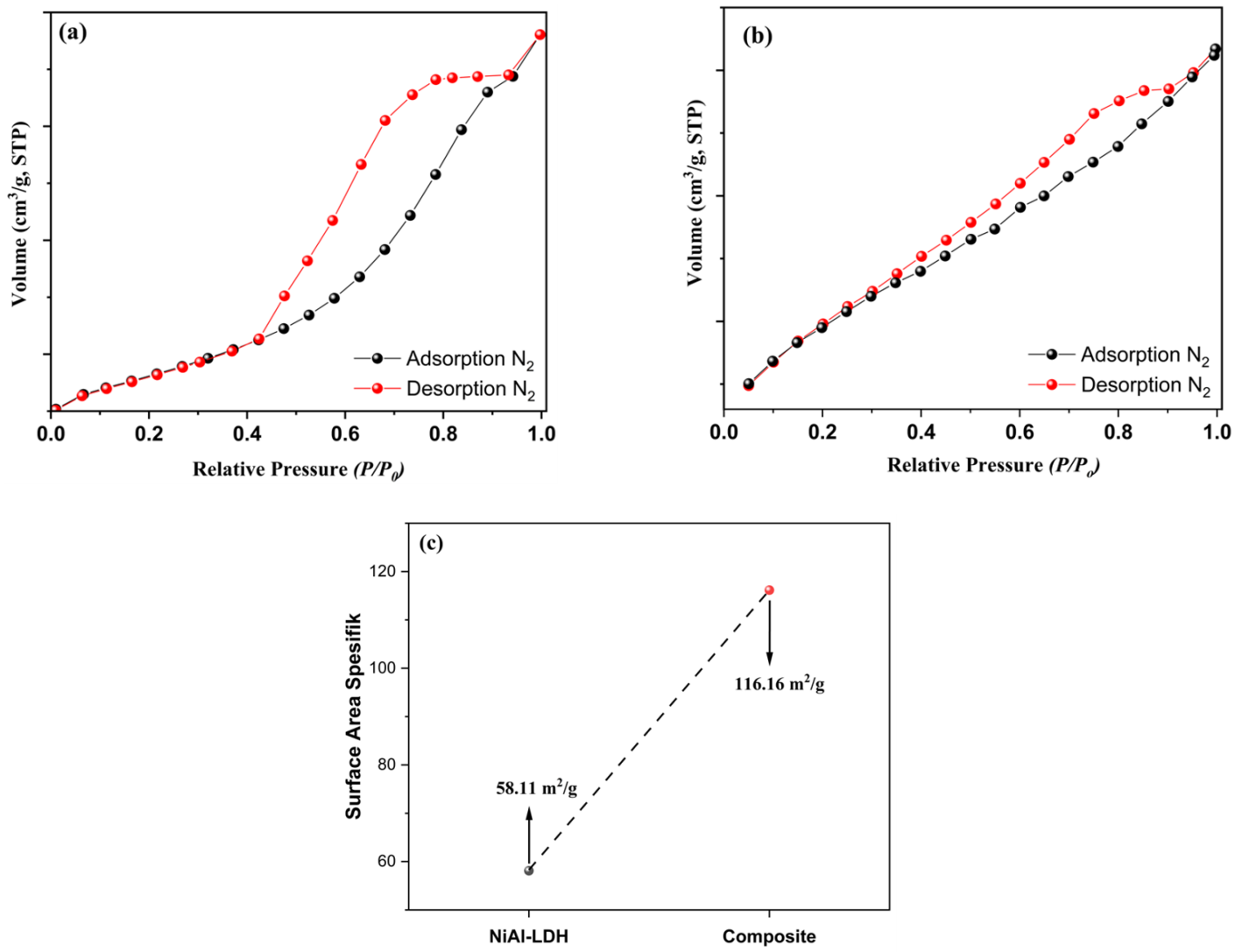

Figure 3. (a) Isotherm of Nitrogen Adsorption-Desorption and Surface Area Specific (b) of NiAl-LDH and NiAl-LDH/$K_4[\alpha\text{-}SiW_{12}O_{40}]$ Composite

determination (R^2) values approaching 1. According to Yazid et al. (2024), a higher R^2 value closer to 1 indicates that the adsorption mechanism aligns with the kinetic analysis data. The R^2 value for NiAl-LDH is 0.991, and for NiAl-LDH/$K_4[\alpha\text{-}SiW_{12}O_{40}]$ composite, it is 0.986. These results suggest that the adsorption of Cr(VI) ions is predominantly governed by chemisorption, which explains that the adsorption process occurs through chemical interactions. The primary mechanism of Cr(VI) metal adsorption involves interactions between the adsorbate and the adsorbent, including complex formation and precipitation.

In the case of Cr(VI) and adsorbents like NiAl-LDH and the NiAl-LDH/$K_4[\alpha\text{-}SiW_{12}O_{40}]$ composite, the chemisorption process involves several steps. These include interactions between functional groups present on the surface of NiAl-LDH or its composite with Cr(VI) metal, the formation of bonds between Cr(VI) ions and the adsorbent surface, the formation of Cr(VI) metal complexes with functional groups on the adsorbent surface, such as interactions with hydroxyl groups (−OH) forming stable complexes, and precipitation Normah et al., 2021a, where Cr(VI) ions react with other components of the adsorbent or ions in the solution, producing insoluble products that precipitate on the adsorbent surface. Data from Table 2 indicate that this chemisorption process is more dominant than physisorption.

3.3 Isotherm Adsorption

The adsorption isotherm experiment was studied through the Langmuir and Freundlich equations (Chen et al., 2022). The adsorption isotherm experiment is conducted to understand how heavy metal Cr(VI) is adsorbed by two types of adsorbent materials: NiAl-LDH and NiAl-LDH/$K_4[\alpha\text{-}SiW_{12}O_{40}]$ composite. This

Table 2. Kinetic Parameters of of NiAl-LDH and NiAl-LDH/$K_4[\alpha\text{-}SiW_{12}O_{40}]$ Composite

Adsorbent	Qe_{exp}	PFO			PSO		
		Q_{calc}(mg/g)	K_1	R^2	Q_{calc}(mg/g)	K_2	R^2
NiAl-LDH	1.688	1.837	0.042	0.933	1.828	0.483	0.991
Composite	2.228	2.726	0.026	0.975	2.514	0.892	0.986

Table 3. Isotherm Parameters of NiAl-LDH and NiAl-LDH/$K_4[\alpha\text{-}SiW_{12}O_{40}]$ Composite

Adsorbent	T(°C)	Langmuir			Freundlich		
		Q_{max} (mg/g)	KL	R^2	n	KF	R^2
NiAl-LDH	60	17.123	0.257	0.972	2.765	7.388	0.997
Composite	60	188.68	0.071	0.988	1.812	4.603	0.998

Table 4. Comparison of Cr(VI) Metal Ions Onto Several Adsorbents

Adsorbent	The Maximum Adsorption Value (mg/g)	Proccess Adsorption	Ref.
Activated carbons	154.56	Monolayer chemisorption	(Wang et al., 2023a)
Fly ash	0.087	-	(Setyawan et al., 2024)
MOF-5	72.12	Monolayer chemisorption	(Babapour et al., 2022)
Fe-MOFs	127.70	physical adsorption	(Miao et al., 2022)
Carboxymethyl chitosan	0.9179	chemisorption	(Nasution et al., 2024)
MOFs nanocomposite	157.23	chemisorption	(Singh et al., 2024)
Copper-Based Metal–Organic Framework	83	-	(Hu et al., 2023)
Mg/Al LDH	30.211	chemisorption	(Siregar et al., 2022)
Humic Acid	3.509	chemisorption	(Siregar et al., 2022)

Table 5. Thermodynamics Data of 25 mg/L Cr(VI) Metal Adsorption Using NiAl-LDH and NiAl-LDH/$K_4[\alpha\text{-}SiW_{12}O_{40}]$ Composite

Adsorbent	ΔH (kJ/mol)	ΔS (J/K.mol)	ΔG (kJ/mol)			
			30°C	40°C	50°C	60°C
NiAl-LDH	9.336	0.042	-3.357	-3.776	-4.194	-4.614
Composite	12.766	0.053	-3.280	-3.809	-4.339	-4.868

data is summarized in Table 3, which includes information on adsorption capacity and isotherm parameters. Data analysis shows that the Freundlich model fits the experimental data better than the Langmuir model, indicated by the correlation coefficient (R^2) values closer to 1. This suggests that adsorption is better described as occurring on a heterogeneous surface with multilayer formation. The Freundlich model implies that Cr(VI) not only adheres to a single layer on the adsorbent surface but forms multiple layers (multilayer) due to the variation in adsorption energy at different sites.

From the data, it can be concluded that Cr(VI) is adsorbed not only through physical mechanisms (physisorption) but also through chemical mechanisms (chemisorption), where chemical bonds form between Cr(VI) and the adsorbent surface. Research by Hung et al. (2023) supports the use of the Freundlich model to describe adsorption on heterogeneous or non-uniform surfaces where there is variation in adsorption bond strength. The parameter n (calculated as 1/nf) reflects the degree of heterogeneity of the adsorbent surface. A high n value indicates a highly heterogeneous surface with varying adsorption intensities. An n value greater than 1 indicates that the adsorption conditions for Cr(VI) on these two types of adsorbents are favourable, with more effective and efficient adsorption (Hu et al., 2023; Wang et al., 2023b).

The trend observed in this study is that the modification of NiAl-LDH with $K_4[\alpha\text{-}SiW_{12}O_{40}]$ significantly increases the adsorption capacity for Cr(VI). The adsorption capacity increased from 17.123 mg/g for NiAl-LDH to 188.68 mg/g for the NiAl-

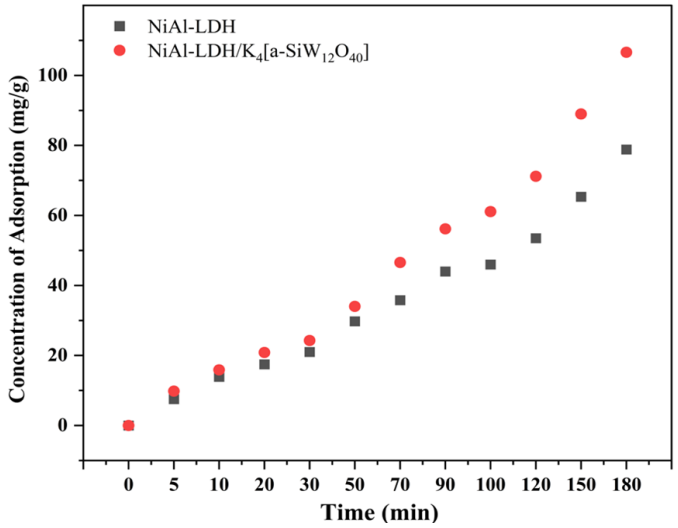

Figure 4. Cr(VI) Ion Adsorption Contact Time Variation Curve

LDH/$K_4[\alpha\text{-}SiW_{12}O_{40}]$ composite, showing a tenfold increase. This demonstrates that the modification is highly effective in enhancing the materials adsorption capability. The adsorption capacity of the NiAl-LDH and NiAl-LDH/$K_4[\alpha\text{-}SiW_{12}O_{40}]$ composite materials can be compared with several other studies that have been carried out and are presented in Table 4.

3.4 Thermodynamic Adsorption

The thermodynamic adsorption study was analyzed using Gibbs energy, enthalpy, and entropy to determine the spontaneity and characteristics of the adsorption process, as shown in Table 5. This study presents thermodynamic findings at different temperature conditions, namely 30, 40, 50, and 60°C. The negative ΔG values observed under all adsorption conditions indicate that the adsorption process is spontaneous (Dhabab, 2011; Yazid et al., 2024). The positive ΔH values show that the adsorption process is endothermic, meaning it requires heat absorption from the surroundings. Meanwhile, the negative ΔS values indicate a decrease in entropy during adsorption, which means that the level of disorder in the system decreases (Dar et al., 2013). This suggests that the adsorbate molecules become more ordered when bound to the adsorbent surface. These findings provide important insights into the fundamental mechanism of the adsorption process and how temperature conditions affect it (Ahmad et al., 2024).

4. CONCLUSIONS

This study successfully synthesized the NiAl-LDH/$K_4[\alpha\text{-}SiW_{12}O_{40}]$ composite composite using the coprecipitation method and evaluated its ability to adsorb Cr(VI) from aqueous solutions. The material characterization showed a significant increase in the specific surface area of the composite compared to pure NiAl-LDH, supporting an enhanced Cr(VI) adsorption capacity. XRD and FT-IR confirmed the successful synthesis and integration of $K_4[\alpha\text{-}SiW_{12}O_{40}]$ composite into the NiAl-LDH structure. At the same time, BET analysis indicated that the specific surface area of the composite doubled compared to pure NiAl-LDH. The adsorption kinetics data indicated that the adsorption process followed the Pseudo-Second-Order (PSO) model with an R^2 value close to 1, suggesting the dominance of chemisorption in the Cr(VI) adsorption mechanism. Isotherm analysis showed that the Freundlich model was more suitable than the Langmuir model, indicating that adsorption occurred on a heterogeneous surface with multilayer formation. The Cr(VI) adsorption capacity of the NiAl-LDH/$K_4[\alpha\text{-}SiW_{12}O_{40}]$ composite composite reached 17.123 mg/g, higher than that of pure NiAl-LDH at 188.68 mg/g.

5. ACKNOWLEDGEMENT

The authors are gratefully acknowledging the Research Center of Inorganic Materials and Complexes at Universitas Sriwijaya for laboratory analysis and assistance, and thankful for Universitas Indo Global Mandiri.

REFERENCES

Ahmad, N., A. Wijaya, F. S. Arsyad, I. Royani, and A. Lesbani (2024). Layered Double Hydroxide-Functionalized Humic Acid and Magnetite by Hydrothermal Synthesis for Optimized Adsorption of Malachite Green. *Kuwait Journal of Science*, **51**(2); 100206

Babapour, M., M. Hadi Dehghani, M. Alimohammadi, M. Moghadam Arjmand, M. Salari, L. Rasuli, N. M. Mubarak, and N. Ahmad Khan (2022). Adsorption of Cr(VI) from Aqueous Solution Using Mesoporous Metal-Organic Framework-5 Functionalized with the Amino Acids: Characterization, Optimization, Linear and Nonlinear Kinetic Models. *Journal of Molecular Liquids*, **345**; 117835

Bai, J., X. Zhang, G. Wang, X. Li, Z. Xu, C. Jing, T. Zhang, and Y. Jiang (2024). The Adsorption-Photocatalytic Synergism of LDHs-Based Nanocomposites on the Removal of Pollutants in Aqueous Environment: A Critical Review. *Journal of Cleaner Production*, **436**; 140705

Boccalon, E., G. Gorrasi, and M. Nocchetti (2020). Layered Double Hydroxides Are Still Out in the Bloom: Syntheses, Applications and Advantages of Three-Dimensional Flower-Like Structures. *Advances in Colloid and Interface Science*, **285**; 102284

Bouali, A. C., M. Serdechnova, C. Blawert, J. Tedim, M. G. S. Ferreira, and M. L. Zheludkevich (2020). Layered Double Hydroxides (LDHs) as Functional Materials for the Corrosion Protection of Aluminum Alloys: A Review. *Applied Materials Today*, **21**; 100857

Boulaiche, W., B. Hamdi, and M. Trari (2019). Removal of Heavy Metals by Chitin: Equilibrium, Kinetic and Thermodynamic Studies. *Applied Water Science*, **9**(2); 1–10

Cao, J., Z. Feng, H. Liang, X. Lu, and W. Wang (2023). Oriented Self-Assembly of Anisotropic Layered Double Hydroxides (LDHs) with 2D-on-3D Hierarchical Structure. *Chemical Engineering Journal*, **472**; 144872

Chen, M., H. Yuan, X. Qin, Y. Wang, H. Zheng, L. Yu, Y. Cai, Q. Liu,

G. Liu, and W. Li (2024). Improve Corrosion Resistance of Steel Bars in Simulated Concrete Pore Solution by the Addition of EDTA Intercalated CaAl-LDH. *Corrosion Science*, **226**; 111636

Chen, X., M. F. Hossain, C. Duan, J. Lu, Y. F. Tsang, M. S. Islam, and Y. Zhou (2022). Isotherm Models for Adsorption of Heavy Metals from Water - A Review. *Chemosphere*, **307**; 135545

Daniel, M., G. Mathew, M. De, and N. Bernaurdshaw (2023). 012 Facets Modulated LDH Composite for Neurotoxicity Risk Assessment through Direct Electrochemical Profiling of Dopamine. *Chemosphere*, **342**; 140177

Dar, B. A., A. Taher, A. Wani, and M. Farooqui (2013). Isotherms and Thermodynamic Studies on Adsorption of Copper on Powder of Shed Pods of *Acacia nilotica*. *Journal of Environmental Chemistry and Ecotoxicology*, **5**(2); 17–20

Daud, M., A. Hai, F. Banat, M. B. Wazir, M. Habib, G. Bharath, and M. A. Al-Harthi (2019). A Review on the Recent Advances, Challenges and Future Aspect of Layered Double Hydroxides (LDH)– Containing Hybrids as Promising Adsorbents for Dyes Removal. *Journal of Molecular Liquids*, **288**; 110989

Deng, Y., Q. Guan, L. He, J. Li, L. Peng, and J. Zhang (2021). The Photothermal Stability of CNFs/ZnAl−LDHs Composited Films: Influence of the Crystal Morphology of ZnAl−LDHs. *Carbohydrate Polymers*, **263**; 117981

Dhabab, J. M. (2011). Removal of Fe(II), Cu(II), Zn(II), and Pb(II) Ions from Aqueous Solutions by Duckweed. *Journal of Oceanography and Marine Science*, **2**(January); 17–22

Ding, G., C. Sun, M. Wang, G. Cheng, J. Liu, and Y. Hu (2024). Effect of Different Metal Ratios on the Synthesis, Morphology and Microwave Absorption Properties of DDM–RGO@$Co_{1-x}Fe_x$–LDH Porous Composites. *Inorganic Chemistry Communications*, **159**; July 2023

Elanchezhiyan, S. S. and S. Meenakshi (2017). Synthesis and Characterization of Chitosan/Mg-Al Layered Double Hydroxide Composite for the Removal of Oil Particles from Oil-in-Water Emulsion. *International Journal of Biological Macromolecules*, **104**; 1586–1595

Farhan, A., A. Khalid, N. Maqsood, S. Iftekhar, H. M. A. Sharif, F. Qi, M. Sillanpää, and M. B. Asif (2024). Progress in Layered Double Hydroxides (LDHs): Synthesis and Application in Adsorption, Catalysis and Photoreduction. *Science of The Total Environment*, **912**; 169160

Gu, Y., Z. Yang, J. Zhou, Q. Fang, X. Tan, and Q. Long (2024). Graphene/LDHs Hybrid Composites Synthesis and Application in Environmental Protection. *Separation and Purification Technology*, **328**; 125042

Hanifah, Y. and A. Amri (2023). Preparation of Layered Double Hydroxide-Polyoxometalate Based Composite. *Indonesian Journal of Material Research*, **1**(2); 68–73

Hu, X., W. Zheng, M. Wu, L. Chen, and S. Chen (2023). Composites of Metal-Organic Frameworks (MOFs) and LDHs for Energy Storage and Environmental Applications: Fundamentals, Progress, and Perspectives. *Sustainable Materials and Technologies*, **37**; e00691

Hung, D. Q., L. X. Dinh, N. Van Tung, L. T. M. Huong, N. T. Lien, P. T. Minh, and T. H. Le (2023). The Adsorption Kinetic and Isotherm Studies of Metal Ions (Co^{2+}, Sr^{2+}, Cs^{+}) on Fe_3O_4 Nanoparticle of Radioactive Importance. *Results in Chemistry*, **6**; 101095

Jiang, Z., M. Wu, P. Gu, W. Huang, C.-P. Yu, Z. Zheng, Y. Wang, N. Yao, and Y. Li (2024). Layered Double Hydroxide@Zeolite Composite Modified Sponge: A Versatile Biocarrier for Enhancing Nitrogen Removal in Biofilters. *Chemical Engineering Journal*, **481**; 148686

Kumari, S., S. Soni, A. Sharma, S. Kumar, V. Sharma, V. S. Jaswal, S. K. Bhatia, and A. K. Sharma (2024). Layered Double Hydroxides Based Composite Materials and Their Applications in Food Packaging. *Applied Clay Science*, **247**; 107216

Latuconsina, H. (2010). Dampak Pemanasan Global Terhadap Ekosistem Pesisir dan Lautan. *Agrikan: Jurnal Ilmiah Agribisnis Dan Perikanan*, **3**(1); 30 (in Indonesia)

Li, T., H. Miras, and Y.-F. Song (2017). Polyoxometalate (*POM*)-Layered Double Hydroxides (LDH) Composite Materials: Design and Catalytic Applications. *Catalysts*, **7**(9); 260

Miao, S., J. Guo, Z. Deng, J. Yu, and Y. Dai (2022). Adsorption and Reduction of Cr(VI) in Water by Iron-Based Metal-Organic Frameworks (Fe-MOFs) Composite Electrospun Nanofibrous Membranes. *Journal of Cleaner Production*, **370**; 133566

Mutahir, S., S. Akram, M. Asim Khan, H. Deng, A. M. Naglah, A. A. Almehizia, M. A. Al-Omar, F. Ibrahim Alrayes, and M. S. Refat (2024). Facile Synthesis of Zn/Co LDH for the Removal of Oxytetracycline from Wastewater: Experimental and *DFT*-Based Analysis. *Chemical Engineering Science*, **283**; 119399

Nasution, D. Y., A. H. Siregar, and E. Rokhmayanti (2024). Determination of Maximum Adsorption Capacity of Chitosan and Carboxymethyl Chitosan on the Absorption of Metal Ions Cr(VI) Based on the Langmuir Equation. *JCNaR Journal of Chemical Natural Resources*, **6**(1); 30–38

Niatouri, A. D. and B. Yadollahi (2023). A Novel *POM*/LDH/GO Nanocomposite as Highly Efficient Heterogeneous Catalyst in Green Epoxidation of Alkenes with Hydrogen Peroxide. *Catalysis Communications*, **185**; 106808

Nie, S., J. Wu, L. Wang, F. Cheng, Z. Sun, X. Chen, H. Liu, S. Wen, and C. Gong (2023). Hierarchical Fe_3O_4@LDH-Incorporated Composite Anion Exchange Membranes for Fuel Cells Based on Magnetic Field Orientation. *Surfaces and Interfaces*, **37**; 102640

Normah, N. R. Palapa, T. Taher, R. Mohadi, H. P. Utami, and A. Lesbani (2021a). The Ability of Composite Ni / Al-Carbon Based Material Toward Readsorption of Iron(II) in Aqueous Solution. *Science and Technology Indonesia*, **6**(3); 156–165

Normah, N. R. Palapa, T. Taher, R. Mohadi, H. P. Utami, and A. Lesbani (2021b). The Ability of Composite Ni/Al-Carbon Based Material Toward Readsorption of Iron(II) in Aqueous Solution. *Science and Technology Indonesia*, **6**(3); 156–165

Palapa, N. R., T. Taher, A. Wijaya, and A. Lesbani (2021). Modification of Cu/cr Layered Double Hydroxide by Keggin Type Polyoxometalate As Adsorbent of Malachite Green from Aqueous Solution. *Science and Technology Indonesia*, **6**(3); 209–217

Qian, J., Y. Zhang, Z. Chen, Y. Du, and B.-J. Ni (2023). NiCo Layered Double Hydroxides/NiFe Layered Double Hydroxides

Composite (NiCo-LDH/NiFe-LDH) Towards Efficient Oxygen Evolution in Different Water Matrices. *Chemosphere*, **345**; 140472

Setyawan, F., F. Dian, I. Sawali, M. A. Afandy, and M. Mustikaningrum (2024). Cr(VI) Removal from Aqueous Solution by Coagulation–Adsorption Integrated System. *Indonesian Journal of Chemical Science*, **13**(1)

Silaen, L., Elfita, R. Mohadi, Normah, N. Juleanti, N. R. Palapa, and A. Lesbani (2021). Soft Ion Divalent Metals toward Adsorption on Zn/Al-POM Layered Double Hydroxide. *Journal of Ecological Engineering*, **22**(10); 109–120

Singh, S., A. G. Anil, B. Uppara, S. K. Behera, B. Nath, N. Pavithra, S. Bhati, J. Singh, N. A. Khan, and P. C. Ramamurthy (2024). Adsorption and DFT Investigations of Cr(VI) Removal Using Nanocrystals Decorated with Graphene Oxide. *Npj Clean Water*, **7**(1); 1–13

Siregar, P. M. S. B. N., A. Wijaya, Amri, J. P. Nduru, N. Hidayati, A. Lesbani, and R. Mohadi (2022). Layered Double Hydroxide/C (C = Humic Acid; Hydrochar) as Adsorbents of Cr(VI) Patimah. *Science and Technology Indonesia*, **7**(1); 41–48

Taher, T., Z. Yu, E. K. A. Melati, A. Munandar, R. Aflaha, K. Triyana, Y. G. Wibowo, K. Khairurrijal, A. Lesbani, and A. Rianjanu (2024). Enabling Dual-Functionality Material for Effective Anionic and Cationic Dye Removal by Using Nb_2O_5/MgAl-LDH Nanocomposites. *Journal of Hazardous Materials Letters*, **5**(October 2023); 100103

Wang, H., W. Wang, S. Zhou, and X. Gao (2023a). Adsorption Mechanism of Cr(VI) on Woody-Activated Carbons. *Heliyon*, **9**(2); e13267

Wang, P., X. Zhang, B. Zhou, F. Meng, Y. Wang, and G. Wen (2023b). Recent Advance of Layered Double Hydroxides Materials: Structure, Properties, Synthesis, Modification and Applications of Wastewater Treatment. *Journal of Environmental Chemical Engineering*, **11**(6); 111191

Wibiyan, S., I. Royani, and A. Lesbani (2024). Selective Adsorption of Cationic and Anionic Dyes Using Ni/Al Layered Double Hydroxide Modified with *Eucheuma cottonii*. *Indonesian Journal of Material Research*, **2**(1); 1–6

Xu, Z., Y. Wu, Z. Zhang, Y. Wang, J. Hu, Y. Ma, Z. Zhang, H. Huang, J. Wei, C. Shi, and Q. Yu (2024). Insight into Ion Exchange Behavior of LDHs: Asynchronous Chloride Adsorption and Intercalated Ions Release Processes. *Cement and Concrete Composites*, **147**; 105433

Yadav, B. S. and S. Dasgupta (2022). Effect of Time, pH, and Temperature on Kinetics for Adsorption of Methyl Orange Dye into the Modified Nitrate Intercalated MgAl LDH Adsorbent. *Inorganic Chemistry Communications*, **137**; 109203

Yazid, H., T. Bouzid, E. M. El Mouchtari, L. Bahsis, M. El Himri, S. Rafqah, and M. El haddad (2024). Insights into the Adsorption of Cr(VI) on Activated Carbon Prepared from Walnut Shells: Combining Response Surface Methodology with Computational Calculation. *Clean Technologies*, **6**(1); 199–220

Zarei, M., T. Ebadi, B. Ramavandi, and S. J. Peighambardoust (2023). Photocatalytic Decomposition of Methylene Blue and Methyl Orange Dyes Using Pistachio Biochar/$CoFe_2O_4$/Mn−Fe−LDH Composite as H_2O_2 Activator. *Surfaces and Interfaces*, **43**; 103571

Zhao, X. J., S. M. Xu, P. Yin, J. Y. Guo, W. Zhang, Y. Jie, and H. Yan (2023). Theoretical Study on the Mechanism of Super-Stable Mineralization of LDHs in Soil Remediation. *Chemical Engineering Journal*, **451**(P1); 138500

